Failure Mechanics—Part II: The Central and Decisive Role of Graphene in Defining the Elastic and Failure Properties for all Isotropic Materials

Richard M. Christensen
Professor Research Emeritus
Aeronautics and Astronautics Department,
Stanford University,
Stanford, CA 94305
e-mail: christensen@stanford.edu

*Continuing from Part I (Christensen, 2014, "Failure Mechanics—Part I: The Coordination Between Elasticity Theory and Failure Theory for all Isotropic Materials," ASME J. Appl. Mech., **81**(8), p. 081001), the relationship between elastic energy and failure specification is further developed. Part I established the coordination of failure theory with elasticity theory, but subject to one overriding assumption: that the values of the involved Poisson's ratios always be non-negative. The present work derives the physical proof that, contrary to fairly common belief, Poisson's ratio must always be non-negative. It can never be negative for homogeneous and isotropic materials. This is accomplished by first probing the reduced two-dimensional (2D) elasticity problem appropriate to graphene, then generalizing to three-dimensional (3D) conditions. The nanomechanics analysis of graphene provides the key to the entire development. Other aspects of failure theory are also examined and concluded positively. Failure theory as unified with elasticity theory is thus completed, finalized, and fundamentally validated.*
[DOI: 10.1115/1.4028407]

Keywords: failure theory, failure mechanics, graphene, elasticity theory

Introduction and Continuation

This work is the continuation of "Failure Mechanics, Part I" [1], now presenting Part II and concluding the sequence. Part I concerned the renormalization of elasticity theory giving it a much simpler and more meaningful (but still rigorous) form that possesses an intimate connection and coordination with failure theory for homogeneous and isotropic materials. The salient results from that work will provide the starting platform for this work.

The program here will be directed toward finalizing the basis for failure theory. There are two major areas of theoretical uncertainty that must be confronted in order to accomplish this. The first question to be resolved concerns the condition required for the relationship between elasticity theory and failure theory to apply. From Part I it is necessary that the Poisson's ratio be non-negative. Although in practice this is a common occurrence, it immediately raises the following question:

> (i) *Is there a physical proof that Poisson's ratio must be non-negative for homogenous and isotropic materials?*

If this cannot be proven then the relationship between elasticity theory and failure theory developed in Part I would become a type of correlation. No doubt a very effective correlation but still far less than the completing keystone on a joint theory of elasticity and failure. Total consistency and compatibility are required for an acceptable failure theory.

This uncertainty about the true nature of Poisson's ratio is one of the oldest completely unsolved issues in all of mechanics. It is not enough to simply declare that Poisson's ratio should always be positive or alternatively to insist that it could be positive or negative. Either claim must be proven for homogeneous and isotropic materials. There are spirited advocates and constituencies for both points of view but no technical proofs either way; that part has always been missing. Further confusion is added by the fact that some anisotropic materials have easily measurable negative Poisson's ratios.

Graphene will be found to have an essential role in resolving the isotropic Poisson's ratio problem with a proof. All of these matters will be explored and treated in considerable detail in the next three sections. The next section recalls the final results from Part I. Then the following third section introduces the fascinating technical area of graphene and ultimately produces the proof that for 2D isotropic elasticity theory the embedded 2D Poisson's ratio must be non-negative. Following and building on the 2D result, the fourth section provides the corresponding proof that 3D theory Poisson's ratio must be non-negative for homogeneous and isotropic materials.

The 2D and 3D proofs are not simple. In both cases the critical reasoning is at the nanoscale. If the problem were easy and direct it would have been archived many ages ago and always promulgated after that. The Poisson's ratio problem is long overdue for resolution. Failure mechanics requires it for its own completion.

The second problem to be faced is the following almost equally fundamental question:

> (ii) *Why is not failure theory best and most generally formulated in terms of the limiting failure stresses in states of shear and dilatation?*

This question is directly motivated by the fact that the kinematics of general states of deformation are prescribed in terms of combinations of states of distortion, states of dilatation and states of rotation. From this it would seem to follow that the associated isotropic failure theory should correspondingly be formulated in terms of failure stresses in shear and in dilatation.

Contributed by the Applied Mechanics Division of ASME for publication in the Journal of Applied Mechanics. Manuscript received August 14, 2014; final manuscript received August 18, 2014; accepted manuscript posted August 27, 2014; published online September 17, 2014. Editor: Yonggang Huang.

The present failure theory is formulated in terms of the failure stresses in uniaxial tension and compression. Uniaxial tensile and compressive failure might appear to be too simplistic, too superficial to anchor a comprehensive, multidimensional theory of materials failure. Thus there could appear to be a basic insufficiency or inconsistency here that must be answered and will be answered in penultimate section.

The resolution to these two fundamental questions related to failure theory will firmly and conclusively place the present failure theory in its proper perspective of generality and completeness. A wide ranging "Summary and Significance" section including important, final assessments will be given at the conclusion of the paper.

3D Theory Results

The main results from Part I [1] will now be recalled for later use here. The failure theory from Refs. [1] and [2] has the polynomial invariants criterion as

$$\left(1-\frac{T}{C}\right)\hat{\sigma}_{ii}+\frac{3}{2}\hat{s}_{ij}\hat{s}_{ij}\le\frac{T}{C} \tag{1}$$

where T and C are the uniaxial tensile and compressive strengths with

$$0\le\frac{T}{C}\le 1 \tag{2}$$

Stress is nondimensionalized by C through

$$\hat{\sigma}_{ij}=\frac{\sigma_{ij}}{C} \tag{3}$$

and the deviatoric stresses are defined by

$$s_{ij}=\sigma_{ij}-\frac{\delta_{ij}}{3}\sigma_{kk} \tag{4}$$

The competitive fracture criterion is specified by

$$\text{If}\quad \frac{T}{C}\le\frac{1}{2} \tag{5a}$$

then

$$\begin{aligned}\hat{\sigma}_1&\le\frac{T}{C}\\ \hat{\sigma}_2&\le\frac{T}{C}\\ \hat{\sigma}_3&\le\frac{T}{C}\end{aligned} \tag{5b}$$

where σ_1, σ_2, and σ_3 are the principal stresses. References [1] and [2] give further details upon the derivation, interpretation and implementation of this two property failure theory.

The renormalized elasticity theory derived in Ref. [1] defines the renormalized Poisson's ratio and renormalized elastic modulus as

$$\nu^*=\frac{3\nu}{1+\nu} \tag{6}$$

and

$$E^*=\frac{E}{1+\nu} \tag{7}$$

The usual positive definite energy requirement provides the standard limits on ν as

$$-1\le\nu\le\frac{1}{2} \tag{8}$$

The possibility of negative values for Poisson's ratio has always been troublesome. Negative values have never been found for homogeneous and isotropic materials, but still their existence has always necessarily been granted and carried forward. Negative values for ν also imply negative values for the renormalized ν^* from Eq. (6).

In the derivation from Ref. [1] it was assumed that Poisson's ratio is always non-negative as

$$0\le\nu\le\frac{1}{2}\quad\text{Assumed} \tag{9}$$

Then the renormalized Poisson's ratio from Eq. (6) has the corresponding range

$$0\le\nu^*\le 1\quad\text{Assumed} \tag{10}$$

Using Eqs. (6) and (7) then the energy and the strain–stress constitutive relations for linear elasticity are given by the concise and compact forms

$$U=\frac{1}{2E^*}\left[3(1-\nu^*)\sigma_M^2+s_{ij}s_{ij}\right] \tag{11}$$

and

$$\varepsilon_{ij}=\frac{1}{E^*}\left[\sigma_{ij}-\nu^*\delta_{ij}\sigma_{\mathrm{M}}\right] \tag{12}$$

where σ_{M} is the mean normal stress.

It also follows that the two renormalized properties are expressible in terms of the shear modulus μ and the bulk modulus k as

$$E^*=2\mu\qquad\nu^*=1-\frac{2\mu}{3k} \tag{13}$$

These two forms should be compared with the more complex classical forms of

$$E=\frac{3\mu}{1+\dfrac{\mu}{3k}}\qquad\nu=\frac{1-\dfrac{2\mu}{3k}}{2\left(1+\dfrac{\mu}{3k}\right)} \tag{14}$$

From Eq. (13) it is seen that E^* directly follows from the shear modulus, but ν^* differentiates the separate sources of distortional and dilatational resistances, through μ and k. This permits a very special interpretation for the renormalized Poisson's ratio, as given in Ref. [1].

With the range on ν^* given by Eq. (10) and that on T/C given by Eq. (2) then the energy constitutive relation (11) and the failure criterion (1) are brought into unification. This permits the definition of a measure of ductility in failure to be defined as

$$D^*=(\nu^*)^2 \tag{15}$$

The ductility property (15) was extensively treated in Ref. [1] and need not be further covered here.

For present purposes, the states of the renormalized elasticity theory and the failure theory are fully integrated with each other. However there is an important and controlling proviso in this relationship. The unification only occurs when Poisson's ratio and correspondingly renormalized Poisson's ratio are non-negative, Eqs. (9) and (10). It will be of first importance to establish whether the non-negative requirement on Poisson's ratio is a fundamental property of mechanical behavior, or simply an idealized and beneficial condition that is usually but not necessarily always satisfied for homogeneous and isotropic materials.

Graphene, 2D Elasticity Theory

In support of the failure theory, the overall objective here is to rigorously prove that Poisson's ratio for homogeneous and isotropic materials can never be negative. But when the best efforts over the past 200 years or so have not succeeded in proving that appealing condition to be true, the task begins to look quite formidable, perhaps even to the point of impossibility. Certainly no straight on, frontal charge at the problem is likely to succeed. All such approaches have already been tried. The only "hope" may be with a more reasoned and balanced approach. Can the problem be broken down into a simpler form that yields to progress and then admits generalization? One such approach is apparent and available.

2D formulations are always more direct and much more simple that 3D formulations. This suggests considering 2D elasticity theory. True 2D elasticity is not a subspace of 3D theory, the latter situation still remains as 3D, just simplified as with plane stress and plane strain. True 2D elasticity immediately suggests the special case of graphene. So the first approach to the Poisson's ratio problem will be to closely examine the 2D elasticity theory that is appropriate to the mechanical characterization of graphene. The introduction of graphene further suggests the involvement of nanomechanics since the special form of graphene can only be described with nanoscale variables. Furthermore, it is far more likely that the physical explanation for non-negative Poisson's ratio is to be found at the nanoscale than at the macroscopic scale.

Accordingly, this section considers the Poisson's ratio problem in the 2D elasticity context appropriate to graphene. Graphene is the carbon based nanostructure that was first synthesized in the form of spherical fullerenes and then later as cylindrical form nanotubes. What is generally accepted as the standard form of graphene is the planar form of the bonding of carbon atoms in a single layer. The essential characteristic is that this layer is only of a single atomic dimension in thickness. Actually it has no easily identifiable thickness in the conventional sense. It is an extraordinary material form, it has the special atomic arrangement having perfect symmetry in its plane, in this case hexagonal symmetry.

Graphene is composed of carbon atoms and no other comparable 2D form is known to exist for any of the other elements. Due to boron's neighboring proximity to carbon in the periodic table and its electronic structure, it might be a candidate for supporting a 2D materials form. But such a boron based material has never been discovered. The carbon form of graphene is unique. It is the only truly 2D form of a materials continuum.

Appropriate to 2D isotropic elasticity theory, the properties must be commensurately defined. With respect to the phantom third direction, one cannot invoke the continuum hypothesis and define a third dimension for thickness identification when the graphene configuration is only one atom in extent. It is not possible to define stress as force per unit area. In 2D theory, stress must be defined as force per unit length. Likewise, the appropriate moduli have units of force per unit length.

The 2-D isotropic elastic moduli and Poisson's ratio are so defined and satisfy the following isotropic condition identities:

$$\begin{aligned}\mu_{2D} &= \frac{E_{2D}}{2(1+\nu_{2D})}\\ K_{2D} &= \frac{E_{2D}}{2(1-\nu_{2D})}\\ E_{2D} &= \frac{4\mu_{2D}K_{2D}}{\mu_{2D}+K_{2D}}\\ \nu_{2D} &= \frac{1-\dfrac{\mu_{2D}}{K_{2D}}}{1+\dfrac{\mu_{2D}}{K_{2D}}}\end{aligned} \tag{16}$$

where K_{2D} is the 2D bulk modulus and the other three properties are similar to those defined in 3D elasticity theory. Any two of the isotropic properties are independent. Only the first identity in Eq. (16) is identical with that from 3D theory. The other three are distinctly different from the 3-D identities.

Next the 2D theory of elasticity will be taken up for later application to graphene, and ultimately to address the Poisson's ratio problem. The stored energy for 2D elasticity is given by

$$U = \frac{1}{2K_{2D}}\left(\frac{\sigma_{ii}}{2}\right)^2 + \frac{1}{4\mu_{2D}}s_{ij}s_{ij}, \quad i,j=1,2 \tag{17}$$

where s_{ij} is the 2D deviatoric stress given by

$$s_{ij} = \sigma_{ij} - \frac{\delta_{ij}}{2}\sigma_{kk}, \quad i,j,k=1,2 \tag{18}$$

The tensor notation ranges over the 2D indices. This convention will always be understood in all the following 2D forms.

Using the identities (16) the energy can be written as

$$U = \frac{(1+\nu_{2D})}{2E_{2D}}\left[\frac{1}{2}\left(\frac{1-\nu_{2D}}{1+\nu_{2D}}\right)\sigma_{ii}^2 + s_{ij}s_{ij}\right] \tag{19}$$

where the limits

$$-1 \le \nu_{2D} \le 1 \tag{20}$$

follow for a positive definite energy form.

Now a renormalization process will be applied similar to that use in Part I [1] of the 3D case. Specifically define the renormalized Poisson's ratio and renormalized elastic modulus by

$$\nu_{2D}^* = \frac{2\nu_{2D}}{1+\nu_{2D}} \tag{21}$$

and

$$E_{2D}^* = \frac{E_{2D}}{1+\nu_{2D}} \tag{22}$$

It follows from Eq. (21) that the limits on ν_{2D}^* are given by

$$-\infty \le \nu_{2D}^* \le 1 \tag{23}$$

If negative Poisson's ratios were not allowed then the limits in Eqs. (20) and (23) would revert to

$$\begin{aligned}0 \le \nu_{2D} \le 1\\ 0 \le \nu_{2D}^* \le 1\end{aligned} \tag{24}$$

However, at this point there is no justification for using Eq. (24) and that leaves Eqs. (20) and (23) as the controlling forms until proven otherwise. In the 3D case, common experience with an enormous range of real materials effectively suggests that negative Poisson's ratio cannot be supported. A justification such as that is not available to be used here in the 2D case. A compelling theoretical reason for disallowing negative 2D Poisson's ratio must be found, if it exists.

The energy form (19) in terms of E_{2D}^* and ν_{2D}^* becomes

$$U = \frac{1}{2E_{2D}^*}\left[\frac{(1-\nu_{2D}^*)}{2}\sigma_{ii}^2 + s_{ij}s_{ij}\right] \tag{25}$$

This can also be written as

$$U = \frac{1}{2E_{2D}^*}\left[2(1-\nu_{2D}^*)\sigma_M^2 + s_{ij}s_{ij}\right] \tag{26}$$

where σ_M is the mean normal stress.

The compatible strain–stress relation is found to be

$$\varepsilon_{ij} = \frac{1}{E^*_{2D}}\left[\sigma_{ij} - \nu^*_{2D}\delta_{ij}\sigma_M\right] \tag{27}$$

These constitutive relations are seen to take extremely simple forms after renormalization.

Using the identities (16) the renormalized properties can be compared with those from the standard 2D elasticity theory. These forms are given by

$$E^*_{2D} = 2\mu_{2D} \quad \nu^*_{2D} = 1 - \frac{\mu_{2D}}{K_{2D}} \tag{28}$$

and

$$E_{2D} = \frac{4\mu_{2D}}{1 + \dfrac{\mu_{2D}}{K_{2D}}} \quad \nu_{2D} = \frac{1 - \dfrac{\mu_{2D}}{K_{2D}}}{1 + \dfrac{\mu_{2D}}{K_{2D}}} \tag{29}$$

Similar to the situation in 3D elasticity, the renormalized properties in Eq. (28) give special interpretations and insights not available through the standard forms (29). In particular the ν^*_{2D} form in Eq. (28) shows how the renormalized Poisson's ratio reflects the distortional and the 2D dilatational stiffness influences. The 2D relations (28) and (29) should be compared with the corresponding 3D relations in Eqs. (13) and (14).

From relation (21) the Poisson's ratios and renormalized Poisson's ratios have the corresponding values

ν_{2D}	0	$\frac{1}{9}$	$\frac{1}{5}$	$\frac{1}{3}$	$\frac{1}{2}$	$\frac{2}{3}$	1
ν^*_{2D}	0	$\frac{1}{5}$	$\frac{1}{3}$	$\frac{1}{2}$	$\frac{2}{3}$	$\frac{4}{5}$	1

A change in direction is necessary now to bring in the nanomechanics of graphene. The hexagonal pattern of atomic positions and bonding is as shown in Fig. 1.

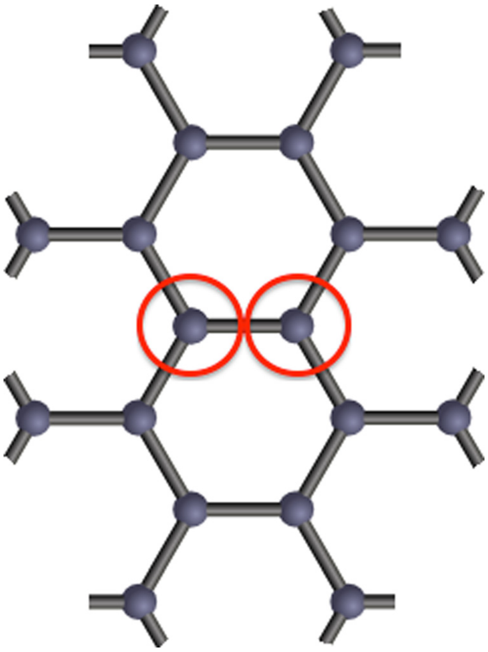

Fig. 1 Hexagonal symmetry for graphene

The carbon atoms in the hexagonal pattern have three nearest neighbors and shared bonding. Following Ref. [2], the nanoscale modeling takes the bonding as represented by joined elastic members spanning across atomic centers and possessing axial and bending stiffness to represent bond stretching and bond bending resistances. The stiffness coefficients are taken as

$$\begin{aligned} k_A &= \frac{A\tilde{E}}{l} \\ k_B &= \frac{12\tilde{E}I}{l^3} \end{aligned} \tag{30}$$

Property $\tilde{E}$ is simply an effective elastic property for the equivalent or hypothetical elastic member.

The elastic member connecting atomic centers is as shown in Fig. 2.

Appropriate to the 2D nature of the problem the thickness of the equivalent elastic member is not needed and the ratio of the stiffness coefficients is then given by

$$\kappa = \frac{k_B}{k_A} = \left(\frac{d}{l}\right)^2 \tag{31}$$

Nanoscale properties κ and d/l have the limits

$$\begin{aligned} 0 \le \kappa \le \infty \\ 0 \le \frac{d}{l} \le \infty \end{aligned} \tag{32}$$

The bending of the equivalent elastic member is taken to be specified by the Bernoulli–Euler theory of bending. The hexagonal pattern of elastic members can be analyzed by enforcing equilibrium of forces and moments at the nodes. This gives closed form solutions for the macroscopic properties of graphene in terms of the nanoscale property κ. The end results are the solutions.

$$\nu_{2D} = \frac{1-\kappa}{1+3\kappa} \tag{33}$$

$$E_{2D} = \frac{4\kappa}{\sqrt{3}(1+3\kappa)}k_A \tag{34}$$

$$\mu_{2D} = \frac{\kappa}{\sqrt{3}(1+\kappa)}k_A \tag{35}$$

$$K_{2D} = \frac{k_A}{2\sqrt{3}} \tag{36}$$

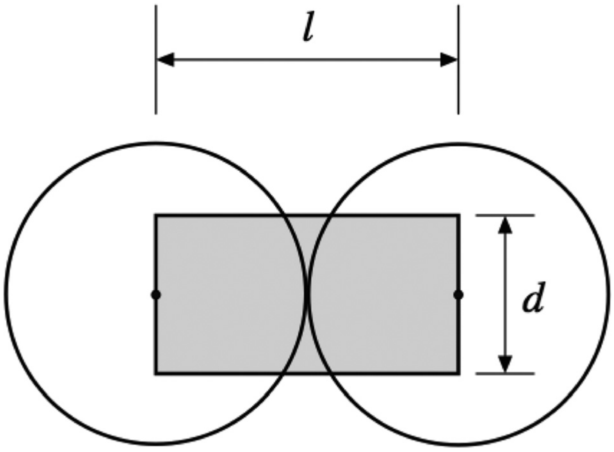

Fig. 2 Effective elastic member connecting carbon atoms

These graphene results are remarkable for their simplicity and clarity. The units of the effective macroscopic moduli are force/unit length.

Taking the limits for κ from Eq. (32), then the limits on Poisson's ratio (33) are

$$-\frac{1}{3} \le \nu_{2D} \le 1 \qquad (37)$$

As an independent check on the results in Eqs. (33)–(37), it can be verified that $\nu_{2D} = -1/3$ allows the hexagonal pattern of elastic members to deform only in extension not in bending at the limit $\kappa \to \infty$. Compared with the 2D elasticity limits in Eq. (20) it is seen that these physical results (37) cut out part of the previously permissible range of negative Poisson's ratios. Still there is a partial range of permissible negative Poisson's ratios. In this sense, some progress has been made, but still it cannot be said that negative Poisson's ratios cannot occur.

There have been many nanoscale models developed of the type shown here. Some of these will be summarized later. None of them give the same results as found here in Eqs. (33)–(36). Furthermore many of them, or perhaps most of them, treat the graphene problem as one having identifiable thickness and employ 3D elasticity theory. This does not by itself mean that they are not correct, but for that reason they do require special interpretation and qualification.

A highly significant relationship follows from these nanomechanics results. Combining Eqs. (31) and (33) gives the very special condition of

$$\nu_{2D} \le 0 \quad \text{when} \quad \frac{d}{l} \ge 1 \qquad (38)$$

Referring to Fig. 2 for interpretation, when *d*/*l* is greater than 1 the Poisson's ratio is negative. This then requires that the size of the effective elastic member extends outside of the atomic dimension of the outer orbital. And for Poisson's ratio significantly less than 0, but satisfying (37) then the effective elastic member extends far outside the atomic dimensions. This is a completely unphysical situation and could not occur in the present conceptual model. Values of *d*/*l* larger than 1 cannot occur, therefore negative values of Poisson's ratio cannot occur.

This is close to the proof that is being sought. The reason that it is not precise and exact is that it cannot be certain that the crossover from acceptability to impossibility occurs exactly at $d/l = 1$. It must be close to that value but perhaps there is a small region of uncertainty immediately near the value $d/l = 1$. Another independent but supporting and reinforcing proof of the unacceptability of negative Poisson's ratio must still be sought.

It is helpful to collect the major results already derived at the nanoscale. Table 1 displays these important results from Eq. (33) for the first row in Table 1 and Eq. (21) gives the second row, along with their inverses.

The first row represents the nanoscale analysis results and the second row the renormalization of the 2D elasticity theory. The third row in Table 1 combines the first two row results to represent the renormalized elastic Poisson's ratio as a function of the nanoscale property κ (31).

Table 1 2D theory relationships between nanoscale and macroscale properties

	Relationship	Inverse
Nanomechanics	$\nu_{2D} = \dfrac{1-\kappa}{1+3\kappa}$	$\kappa = \dfrac{1-\nu_{2D}}{1+3\nu_{2D}}$
Renormalization	$\nu_{2D}^* = \dfrac{2\nu_{2D}}{1+\nu_{2D}}$	$\nu_{2D} = \dfrac{\nu_{2D}^*}{2-\nu_{2D}^*}$
Combination	$\nu_{2D}^* = \dfrac{1-\kappa}{1+\kappa}$	$\kappa = \dfrac{1-\nu_{2D}^*}{1+\nu_{2D}^*}$

Yet another special behavior is now evident in Table 1. The two expressions in the third row are identical in form. That is, the interchange of the two symbols ν_{2D}^* and κ does not alter the functional forms relating them. The two variables ν_{2D}^* and κ are mathematical duals. This is a special and unusual relationship. The two inverse forms are also dual forms relating the macroscopic variable ν_{2D}^* and the nanoscale variable κ. It can be noted that the same dual relationship occurs in the first row of Table 1, but it is this behavior with the renormalized Poisson's ratio in the third row that is the most significant. This latter 2D theory result will be found to relate to a similar behavior in the 3D case in the next section and be of decisive use there.

Now everything is arranged and ready for the final result and conclusion in the 2D case for graphene. The relationship between ν_{2D}^* and the nanoscale property κ, is shown in Fig. 3.

The horizontal axis κ in Fig. 3 is the ratio of the bond bending stiffness to the bond stretching stiffness (31) so the κ axis cannot take negative values, as shown. But because ν_{2D}^* and κ are duals, the axes in Fig. 3 can be interchanged and therefore both κ and ν_{2D}^* cannot be negative, also as shown in Fig. 3. This is the final proof that ν_{2D}^* and thereby ν_{2D} cannot take on negative values.

This is the conclusive nanomechanics proof that Poisson's ratio for graphene or any other potential 2D elastic material with covalent, hexagonal bonding cannot have negative Poisson's ratio.

It will also be of interest to determine the explicit value of Poisson's ratio for graphene, and that will be done in a later section. But at this point that is of secondary importance compared with proving that graphene's Poisson's ratio cannot be negative. It is that special result that will provide guidance on how to proceed with the 3D question of whether Poisson's ratio can or cannot take on negative values. The answer to that question will have far reaching implications for the validity of the related failure theory.

3D Theory Proof

For 3D theory the missing information is why Poisson's ratio never seems to be negative for homogeneous and isotropic materials. Is that a fundamental physical requirement or is it simply an extremely common occurrence? The same question was posed for 2D elasticity theory, for application to graphene, and it was found

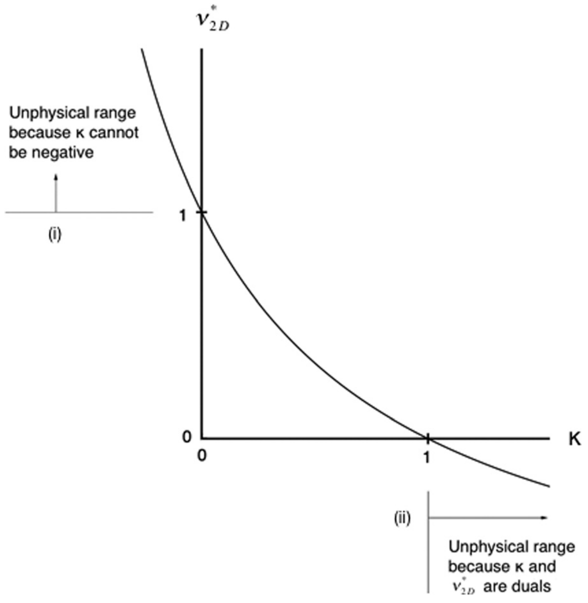

Fig. 3 **2D ν_{2D}^* versus κ, Table 1**

and proven in the previous section that 2D Poisson's ratio cannot be negative, it is an absolute physical restriction that it be zero or positive. Is there a simple carryover from 2D to 3D that can be applied here? Unfortunately there is no such simple extension of the 2D proof to answer the 3D question. If the non-negative proposition cannot be proven for the 3D case then the connection between elasticity theory and failure theory becomes less strong, less physically meaningful.

A rigorous nanomechanics analysis was used to prove the condition $\nu_{2D} \geq 0$. A comparably rigorous nanoscale analysis cannot be performed in the 3D case. The 2D hexagonal symmetry of the atomic arrangement for graphene has no counterpart for the 3D case that can assure isotropy. The condition of isotropy in 3D is that of six axes of fivefold symmetry. There is no periodic arrangement of single type cells with the necessary symmetry that packs in 3-space. So the problem cannot be approached in exactly the same manner that succeeded in 2-space. However, the 2D proof is still invaluable and it will be shown to generally and broadly guide the way in the much more complicated 3D case. The outline here follows that in Ref. [2] but goes further to a decisive conclusion.

Postulate the existence of a nanoscale variable that represents the ratio of the bond bending resistance to the bond stretching resistance in 3D conditions as

$$\hat{\kappa} = \frac{k_B}{k_A} \tag{39}$$

Going further, postulate a relationship between Poisson's ratio ν and $\hat{\kappa}$ of the same form as in the 2D case, (33), thus

$$\nu = \frac{1 - \alpha\hat{\kappa}}{\beta + \gamma\hat{\kappa}} \tag{40}$$

where α, β, and, γ are to be determined. The first two conditions to be used for this purpose are that

$$\begin{aligned} \nu &= -1 \quad \text{at} \quad \hat{\kappa} \to \infty \\ \nu &= \frac{1}{2} \quad \text{at} \quad \hat{\kappa} = 0 \end{aligned} \tag{41}$$

These are the standard limits.

The third condition comes from rescaling $\hat{\kappa}$ such that $\kappa = (4/3)\hat{\kappa}$ then gives

$$\nu = 0 \quad \text{at} \quad \kappa = 1 \tag{42}$$

Ref. [2] gives the details. Conditions (41) and (42) determine Eq. (40) to take the form

$$\nu = \frac{1 - \kappa}{2 + \kappa} \tag{43}$$

This nanoscale motivated analysis has the specific 3D result (43) comparable to the 2D result (33). Relation (43) cannot be considered to be perfectly rigorous because it does not come from a nanomechanics analysis of a particular arrangement of atomic bonding between neighboring atoms. But it does follow as the same general methodology as in the rigorous 2D case.

One more result from this derivation must be cited. The bonding arrangement between atoms was taken the same as in Fig. 2 for the 2D case but now the dimension d refers to the diameter of the effective circular cylindrical effective elastic member connecting neighboring atoms. It follows that the imposed condition (42) can equivalently be stated here as

$$\nu = 0 \quad \text{at} \quad \frac{d}{l} = 1 \tag{44}$$

where it can be shown that with the rescaling then

$$\kappa = \left(\frac{d}{l}\right)^2 \tag{45}$$

The difference between the present results and those of the 2D case is that in the 2D case the result (44) was the outcome of the nanoscale analysis whereas here it was used in the form of Eq. (42) to deduce the main result (43).

Now these results will temporarily be held in place while the renormalization of elasticity theory results is recalled. Nothing yet is sufficient to argue the main question on the form of ν, but the necessary pieces are being assembled.

First, recall the renormalized forms for the 2D energy and strain–stress relations from Eqs. (26) and (27), but now as stated with the knowledge that Poisson's ratio cannot be negative

$$\left.\begin{aligned} U &= \frac{1}{2E^*_{2D}}\left[2\left(1-\nu^*_{2D}\right)\sigma_{\mathrm{M}}^2 + s_{ij}s_{ij}\right] \\ \varepsilon_{ij} &= \frac{1}{E^*_{2D}}\left[\sigma_{ij} - \nu^*_{2D}\delta_{ij}\sigma_{\mathrm{M}}\right] \end{aligned}\right\} 2\text{–}D, \quad 0 \leq \nu^*_{2D} \leq 1 \tag{46}$$

The corresponding 3D results from Eqs. (11) and (12) are

$$\left.\begin{aligned} U &= \frac{1}{2E^*}\left[3(1-\nu^*)\sigma_{\mathrm{M}}^2 + s_{ij}s_{ij}\right] \\ \varepsilon_{ij} &= \frac{1}{E^*}\left[\sigma_{ij} - \nu^*\delta_{ij}\sigma_{\mathrm{M}}\right] \end{aligned}\right\} 3\text{–}D \tag{47}$$

Note that the Poisson's ratio restriction in Eq. (46) as yet has no counterpart in Eq. (47). Comparing the 2D constitutive forms (46) with the 3D constitutive forms (47) they are seen to be virtually identical. The only differences are in the factors of 2 that enter (46) versus the factors of 3 that enter (47). These differences are directly from the 2D versus the 3D formulations. This comparison of 2D and 3D constitutive forms strongly suggests that because one set, (46), cannot allow negative Poisson's ratios it is very likely that the other set, (47), must also be similarly restricted. Suggestive though this may be, it still is not a proof. It still must be proven that 3-D Poisson's ratio cannot be negative. However everything is now in place to complete the last step in the proof.

Corresponding to Table 1 for the 2D proof, the main results for the 3D case are assembled in Table 2.

The first row in Table 2 is from Eq. (43) and its inverse form relating ν and the nanoscale property κ. The second row is the renormalized Poisson's ratio as related to the classical form, namely Eq. (6). Finally the third row results come from the combination of the first two row forms.

As with the 2D results in Table 1, a special result emerges in the Table 2 forms. The relationship between macroscopic Poisson's ratio ν^* and the nanoscale property κ is that the form and its inverse are identical. That is, the interchange of the symbols ν^* and κ produces a form that is unchanged and identical with its inverse. Properties ν^* and κ are mathematical duals. The same duality property cannot be said of the relationship between ν and

Table 2 3D theory relationships between nanoscale and macroscale properties

	Relationship	Inverse
Nanomechanics	$\nu = \frac{1-\kappa}{2+\kappa}$	$\kappa = \frac{1-2\nu}{1+\nu}$
Renormalization	$\nu^* = \frac{3\nu}{1+\nu}$	$\nu = \frac{\nu^*}{3-\nu^*}$
Combination	$\nu^* = 1-\kappa$	$\kappa = 1-\nu^*$

κ in the first row of Table 2. This is the power of the renormalization methodology for elasticity theory.

Finally, the relationship between ν^* and κ in Table 2 is as shown in Fig. 4.

From the definition of $\hat{\kappa}$ and thereby κ the nanoscale property must be positive, κ is the ratio of the bond bending stiffness to the bond stretching stiffness. With the requirement of non-negative κ and the dual nature of κ and ν^* it follows that ν^* must also be non-negative. To say this other way, properties ν^* and κ can be interchanged without altering the functional interdependence between them. Since κ must be non-negative it follows that so too renormalized Poisson's ratio must be non-negative. The end result is that

$$0 \le \nu^* \le 1 \quad \text{Proved} \tag{48}$$

$$0 \le \nu \le \frac{1}{2} \quad \text{Proved} \tag{49}$$

These are the same as in Eqs. (9) and (10) except that there they were assumed, here they are proved. A requirement of positive macroscopic energy was not used in this nanoscale proof, although it certainly is satisfied.

For full density, homogeneous and isotropic materials that satisfy the condition (2) on the failure properties T and C, then the condition (48) on ν^* provides the compatibility between the failure theory and the renormalized elasticity theory. In the present context, the term homogeneous means that the elastic behavior is controlled by features at the nanoscale, not at the macroscopic scale. From this proof it is seen that negative values of Poisson's ratio require physically unrealistic, absurdly large values of the bond bending resistance compared with the bond stretching resistance.

2D and 3D Theory Consequences

It is of some interest to go a little further with relevant property values. To finish this treatment of 2D graphene and 3D theory, it is of explicit interest to determine the Poisson's ratio for graphene. Since graphene is the pure form of the carbon atom in 2D, it is equally important to examine the corresponding property for the carbon atom in 3D, namely, for diamond. Ideally, it would be advantageous to start with the Poisson's ratio for diamond and then incorporate that into the present theoretical results to predict the Poisson's ratio for graphene and compare that with reported values.

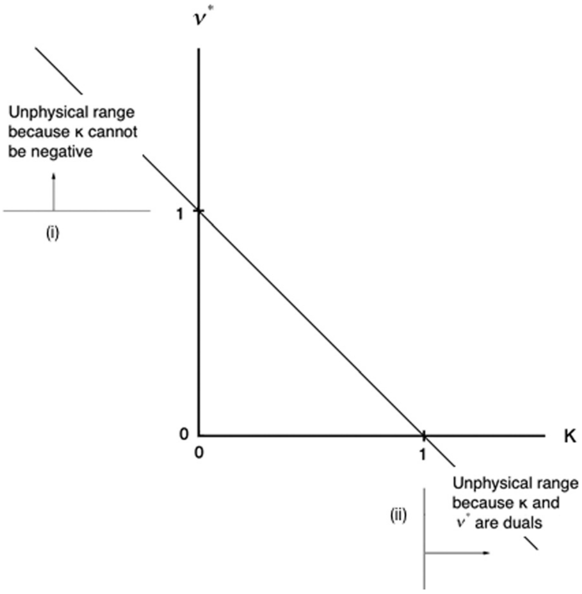

Fig. 4 **3D ν^* versus κ, Table 2**

It is somewhat surprising to find that the Poisson's ratio value for polycrystalline diamond is not well established and standardized. Its determination is still a quite controversial subject. Measured values are claimed that range from $\nu = 0.07$ up to quite large values in the range from 0.3 to 0.4. Theoretical predictions based upon single crystal anisotropic properties also have an enormous range of predicted values. However, by far the most commonly reported experimental value is that of $\nu = 0.2$. The apparently more realistic values are those reported for so called amorphous diamond, as with those in thin film technology. The most reliable measurements appear to be those from S. Cho et al. [3] and S.-J. Cho et al. [4]. Reference [3] measure is $\nu = 0.17 \pm 0.03$ and that of Ref. [4] is $\nu = 0.22$. Other related references are those of Robertson [5], Greaves et al [6], and Spear and Dismukes [7]. The Poisson's ratio for polytcrystalline diamond, based upon these most commonly reported values, will here be taken as

$$\nu = \frac{1}{5} \quad \text{Diamond} \tag{50}$$

Now, attention is turned to graphene. The Poisson's ratio for graphene can be determined from that for single wall nanotubes. For nanotubes the two atomic configurations of "zigzag" and "armchair" have different expected values for their Poisson's ratios, but they converge together as the diameter of the nanotube increases. As with diamond, there is a very wide range of predicted values for Poisson's ratio of graphene. Related references are Chang and Gao [8], Popov et al. [9], Tu and Yang [10], Li and Chou [11], Treacy et al. [12], Zhao and Shi [13], and Scarpa et al. [14]. The major works by Chang and Gao [8] and Popov et al. [9] are the most definitive. The former predicts the Poisson's ratio of graphene as 0.16 and the latter as 0.212. The other reported theoretical predictions for ν_{2D} of graphene range from about 0.125 to 0.85.

The ideal theoretical prediction of the in-plane properties of graphite has been given by Al-Jishi and Dresselhaus [15], which material form is intimately related to that of graphene. Explicit values for Poisson's ratio were not given. The measured value of Poisson's ratio for graphene by Lee et al. [16] is $\nu_{2D} = 0.165$. The predicted and measured values of Poisson's ratio for graphene, although scattered broadly, are fairly well centered on the value of $\nu_{2D} = 0.20$ or a little less.

Next the prediction for the Poisson's ratio of graphene from the present results will be given. The starting point is the Poisson' ratio of diamond at the value $\nu = 1/5$, (50), as discussed earlier. From Table 2 the corresponding value for the nanoscale property κ for diamond is then

$$\kappa = \left.\frac{1 - 2\nu}{1 + \nu}\right|_{\nu = \frac{1}{5}} = \frac{1}{2} \quad \text{Diamond} \tag{51}$$

This is the effective ratio of the 3D bond bending stiffness to the bond stretching stiffness. Since this is the intrinsic property for the carbon atom, the same value of $\kappa = 1/2$ will be taken for κ in the 2D case of graphene. From Table 1 the Poisson's ratio of graphene is then given by

$$\nu_{2D} = \left.\frac{1 - \kappa}{1 + 3\kappa}\right|_{\kappa = \frac{1}{2}} = \frac{1}{5} \quad \text{Graphene} \tag{52}$$

Thus diamond and graphene are here predicted to have about the same Poisson's ratio of 1/5. This is in reasonable accord with practice, as already discussed. The corresponding renormalized Poisson's ratios are $\nu^* = 1/2$ and $\nu^*_{2D} = 1/3$.

Before leaving this extensive and intensive examination of Poisson's ratio, for both general and specific cases, one final related matter should be discussed. Although this is the first and only proof that Poisson's ratio cannot be negative for homogeneous and isotropic materials, there have been many studies over history on various other aspect of this unusual and poorly understood nondimensional property. For example, Mott and Roland [17] purport to prove that "classical elasticity is inapplicable whenever $\nu < 1/5$." At the other extreme, negative values of Poisson's ratio have been reported for so called "auxetic" materials [6]. But these are porous materials and thereby not homogeneous. They lie outside the range of present considerations. Poisson's ratio has always been something of a mystery property. Its true significance should finally be understood and utilized.

Much of what has been done here revolves around graphene and makes use of its very special properties. At the level of a continuum of atoms in 2D it very likely is the perfect material. Although it is unique in this sense, it is almost ridiculously common in another sense. Graphite is simply the common macroscale form of graphene. Necessarily graphite exists only with dominant flaw and defect substructures. Graphite is extremely useful as a solid lubricant and for a variety of other things. However, "low-tech" graphite can be converted to some very specialized "high-tech" applications.

With heat and pressure, randomly oriented grains of graphite can be formed into very special materials having considerable structural integrity. The flame exposed surface of rocket nozzles is one such example of a graphitic material that must withstand severe heat environments. For that purpose Ely [18] has tested the strength properties of fused graphite. The present failure theory can be compared with the biaxial stress testing data, Fig. 5.

The theoretical predictions are from Eqs. (1) and (5). T and C are taken as

$$T = 3800\,\text{psi} = 26.2\,\text{MPa}$$
$$C = 10,000\,\text{psi} = 68.9\,\text{MPa}$$

The fracture cutoff effect is fairly prominent in Fig. 5 even though the T/C ratio is only slightly smaller than 1/2.

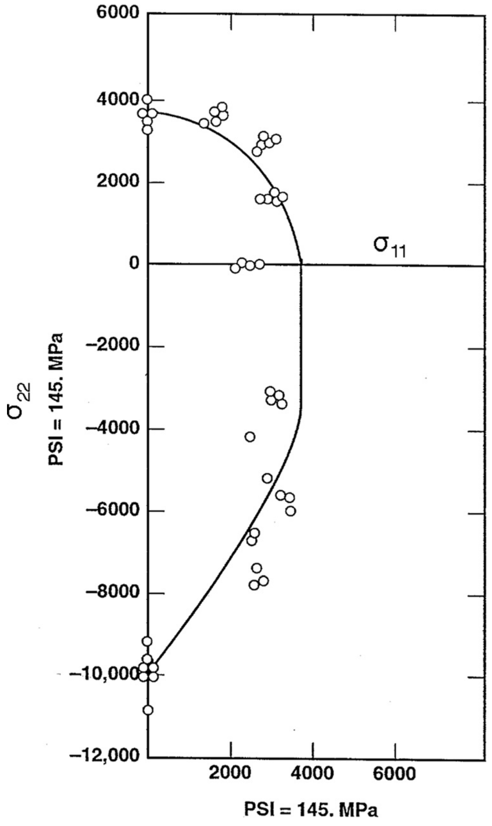

Fig. 5 Biaxial failure data for fused graphite, Ely [18]

If all the major data groupings in Fig. 5 were fitted by unphysical, blind polynomial forms, the resulting envelope would contain concave as well as convex portions. That behavior is not possible in the present physical context. The reality of fitting failure data often (usually) involves taking best fits, far short of perfection. Such is the case here. Often the data scatter and inconsistency is due to batch to batch variations in preparing test specimens. Failure measurements are acutely sensitive to this complication, much more so than are elastic modulus measurements. Nevertheless, the comparison in Fig. 5 is reasonable and this graphite example fits in with all the other widely different materials examples shown in the previous verification examinations for this failure theory.

Distortion and Dilatation

The second question posed in the "Introduction and Continuation" section will now be taken up. What is the most effective and most efficient way to calibrate a general theory of failure? Most would say that the best way to proceed would be through the failure stresses in states of shear and dilatation. The present theory uses the failure stresses in uniaxial tension and compression. Another way to pose the question is to suggest or infer that it may seem to some to be unlikely that a comprehensive failure theory intended for applications having multidimensional stress fields could be completely specified by and anchored by only data from uniaxial failure.

To resolve this issue of the proper basis for failure theory, it is convenient to start with the present failure theory given by Eqs. (1) and (5). These are completely calibrated by T and C. Following and amplifying Ref. [2], consider how these forms would appear if calibrated by failure in simple shear, S, and by positive dilatation failure, D^+. Using Eq. (1) it is found that S and D^+ are specified by

$$S^2 = \frac{TC}{3} \tag{53}$$

$$D^+ = \frac{TC}{3(C-T)} \tag{54}$$

These can be inverted to give T and C in terms of S and D^+ as

$$T = \frac{S^2}{2D^+}\left[-1 + \sqrt{1 + 12\left(\frac{D^+}{S}\right)^2}\right] \tag{55}$$

$$C = \frac{S^2}{2D^+}\left[1 + \sqrt{1 + 12\left(\frac{D^+}{S}\right)^2}\right] \tag{56}$$

The polynomial invariants criterion (1) would then be given by

$$\frac{(\hat\sigma_1 + \hat\sigma_2 + \hat\sigma_3)}{3D^+} + \frac{1}{6S^2}\left[(\hat\sigma_1 - \hat\sigma_2)^2 + (\hat\sigma_2 - \hat\sigma_3)^2 + (\hat\sigma_3 - \hat\sigma_1)^2\right] \le 1 \tag{57}$$

where principal stress notation is used. Comparing Eqs. (1) and (57), it is seen that this failure criterion is perfectly well and effectively specified in terms of failure in shear, S, and in positive dilatation, D^+.

It remains to consider the fracture criterion (5) in terms of S and D^+. It is found that with σ_1 being the largest principal stress (5) becomes

$$\sigma_1 \le \frac{S^2}{2D^+}\left[-1 + \sqrt{1 + 12\left(\frac{D^+}{S}\right)^2}\right] \quad \text{if} \quad \frac{D^+}{S} \le \sqrt{\frac{2}{3}} \tag{58}$$

The T/C term in Eq. (5), when using Eqs. (55) and (56), ultimately reduces to the form in Eq. (58).

Here is where the difficulty arises. The fracture criterion (58) in terms of S and D^+ is rigorously the same as Eq. (5) but physically it is total nonsense. In the form in Eq. (58) it loses all identification with a fracture event controlled by the largest positive principal stress.

In another example, Ref. [2] gives a method for determining the ductile brittle transition for all materials types in any stress state. For simple tension the D/B transition is given by

$$\begin{aligned} \frac{T}{C} &< \frac{1}{2} \quad \text{Brittle} \\ \frac{T}{C} &> \frac{1}{2} \quad \text{Ductile} \end{aligned} \tag{59}$$

This D/B criterion is very easily interpreted and verified with commonly available data. In contrast, for the state of simple shear, the D/B criterion in terms of S and D^+ is found to be given by

$$\begin{aligned} \frac{D^+}{S} &< \frac{1}{2} \quad \text{Brittle} \\ \frac{D^+}{S} &> \frac{1}{2} \quad \text{Ductile} \end{aligned} \tag{60}$$

This result is difficult to interpret and in terms of practical utility, it is virtually useless

In response to the criticisms just given, a rejoinder could say, yes but these forms start with the forms of the present failure theory. What if a new theory were developed entirely in terms of shear and dilatation failure. Of course it is totally speculative to suggest what form such a theory would take, but it is likely that it would arrive at something very much like the form in Eq. (57), if not identical with it. This is not only because the form in Eq. (57) is calibrated by S and D^+ but also because the two individual terms in Eq. (57) are explicitly those of positive dilatation for the first term and pure distortion for the second term.

A two property failure theory expressed purely in terms of shear and positive dilatation could hardly arrive at anything except something similar to Eq. (57). This would then completely omit the presence of the fracture criterion, Eq. (5). The consequence of this omission would be an incomplete failure theory. The brittle limit given by $T/C = 0$ in the present theory (with profound implications) would have no counterpart in the purely distortion and dilatation theory. Looking to the next step beyond this first conclusion, it also follows that the ductile brittle transition and related developments defined in the present theory would have no counterpart in the hypothetical theory based only on distortion and dilatation.

It is necessary that a general two property failure theory be formulated with one part involving the interactive shear/dilatation mechanism and the other part a competitive criterion representing a fracture mechanism. Such a theory could only be formulated in terms of uniaxial tensile and compressive failures. Uniaxial strengths T and C comprise the most fundamental form of the material failure specification for homogeneous and isotropic materials.

Summary and Significance

It is not just a coincidence that the present theory of failure is fully specified by just two properties of failure, the same as the number of independent elastic constants for homogeneous and isotropic materials. The explicit connection between elasticity theory and failure theory was established and discussed at length in Part I [1] of this work. That relationship coordinates completely with the manner of derivation of the failure theory [2], which was based upon viewing failure as the termination of the elastic range of behavior, even when plasticity occurs. Nevertheless one specific and crucial assumption was required in order to obtain the comprehensive theory. That same assumption or uncertainty has been an enduring problem every since the conception and early development of elasticity theory by the founders of physical science.

The critical underlying assumption of Part I was that of the positive values for Poisson's ratio. If Poisson's ratio could be negative then the entire connection between elasticity theory and failure theory would reduce to only that of a correlation. Accordingly, this Part II of the study has been committed to proving the efficacy of non-negative and only non-negative Poisson's ratios for homogeneous and isotropic materials. This proof was accomplished through the conjunction of two unusual developments. First, classical elasticity theory was renormalized to give a special form revealing basic behaviors, especially that of renormalized Poisson's ratio.

The second development was a nanoscale analysis of graphene giving closed form analytical solutions for the associated elastic properties. The 2D renormalized elasticity theory when combined with the nanomechanics analysis yielded the proof that 2D Poisson's ratio cannot be negative. This assurance of consistent mechanical behavior at the 2D level then led to a generally similar proof of existence for only non-negative 3D Poisson's ratios. The resulting unified theory of elasticity and theory of failure is now consistent and compatible in all respects.

The key mechanics result that made this possible was the 2D elasticity theory as applied to the characterization of graphene. As a material architecture at the nanoscale, graphene is not only unique, it is sublime. It possesses the perfect nanostructure and that allows nearly perfect mechanical behavior. Positive Poisson's ratio is an important and integral and necessary part of graphene's many attributes.

In related matters, it also is no surprise that the proof of non-negative values of 2D and 3D Poisson's ratios for homogeneous and isotropic materials was consummated at the nanoscale, not at the macroscale. It very likely could not be accomplished at the macroscopic scale.

With the proof that Poisson's ratio must be non-negative, it is now obvious that E and ν are the fundamental elastic properties, not μ and k. The shear modulus and bulk modulus have more restrictive ranges than they would otherwise have. Furthermore, with this result it is also transparently clear why T and C as conjugates to E and ν are the corresponding fundamental failure forms.

For general materials, the occurrence of plasticity behavior as an interim passage between initial yield and effective failure does not upset any of the associations already discussed. The method by which failure is defined in Chap. 9 of Ref. [2] allows ample latitude for plasticity in between the elastic range and effective failure.

For many different reasons the two calibrating properties for the failure theory were found to be those of the uniaxial tensile and compressive strengths. They were not casually adopted simply because of their obvious convenience. The basis of their use was totally different from that. Going even further, it would be justified to say that the failure theory would not have been possible without the involvement of the materials failure identifier T/C. The brittle limit at $T/C = 0$ very likely would have remained a vague and elusive and ill defined concept without the T/C involvement. That the T/C ratio would be found to admit characterization as the ductility index for simple tension could not have even been imagined. But these results and much more were the normal and natural outcomes when the T/C based failure theory was assembled and functioning. The T/C identification and the theoretical relationship between elasticity and failure provided the essential and probably unique capability for the failure methodology.

This final synthesis of combined elasticity and failure theories completes the foundation for failure theory and provides the general basis for the failure mechanics of homogeneous and isotropic materials.

Acknowledgment

The author is appreciative of support for this work from the Office of Naval Research, Dr. Y. D. S. Rajapakse, Program Manager.

References

[1] Christensen, R. M., 2014, "Failure Mechanics—Part I: The Coordination Between Elasticity Theory and Failure Theory for all Isotropic Materials," ASME J. Appl. Mech., **81**(8), p. 081001.

[2] Christensen, R. M., 2013, *The Theory of Materials Failure*, Oxford University, Oxford, UK.

[3] Cho, S., Chasiotis, I., Friedman, T. A., and Sullivan, J. P., 2005, "Young's Modulus, Poisson's Ratio and Failure Properties of Tetrahedral Amorphous Diamond-Like Carbon for MEMS Devices," J. Micromech. Microeng., **15**(4), pp. 728–735.

[4] Cho, S.-J., Lee, K.-R., Eun, K. Y., Hahn, J. H., and Ko, D.-H., "Determination of Elastic Modulus and Poisson's Ratio for Diamond-Like Carbon Films," Thin Solid Films, **341**(1–2), pp. 207–210.

[5] Robertson, J., 2002, "Diamond-Like Amorphous Carbon," Mater. Sci. Eng., **37**(4–6), pp. 129–281.

[6] Greaves, G. N., Greer, A. L., Lakes, R. S., and Rouxel, T., 2011, "Poisson's Ratio and Modern Materials," Nat. Mater., **10**(11), pp. 823–837.

[7] Spear, K. E., and Dismukes, J. P., 1994, *Synthetic Diamond*, Wiley, New York.

[8] Chang, T., and Gao, H., 2003, "Size-Dependent Elastic Properties of a Single-Walled Carbon Nanotube Via a Molecular Mechanics Model," J. Mech. Phys. Solids, **51**(6), pp. 1059–1074.

[9] Popov, V. N., van Doren, V. E., and Balkanski, M., 2000, "Elastic Properties of Single-Walled Carbon Nanotubes," Phys. Rev. B, **61**(4), pp. 3078–3084.

[10] Tu, Z. C., and Yang, Z.-C., 2002, "Single-Walled and Multiwalled Carbon Nanotubes Viewed as Elastic Tubes With the Effective Young's Modulus Dependent on Layer Number," Phys. Rev. B, **65**(23), p. 233407.

[11] Li, C., and Chou, T.-W., 2003, "A Structural Mechanics Approach for the Analysis of Carbon Nanotubes," Int. J. Solids Struct., **40**(10), pp. 2487–2499.

[12] Treacy, M. M. J., Ebbesen, T. W., and Gibson, J. M., 1996, "Exceptionally High Young's Modulus Observed for Individual Carbon Nanotubes," Nature, **381**(6584), pp. 678–680.

[13] Zhao, P., and Shi, G., 2011, "Study of Poisson's Ratios of Graphene and Single-Walled Carbon Nanotubes Based on an Improved Molecular Structural Mechanics Model," TechScience, **5**(1), pp. 49–58.

[14] Scarpa, F., Adhikari, S., and Phani, A. S., 2009, "Effective Elastic Mechanical Properties of Single Layer Graphene Sheets," Nanotechnology, **20**(6), pp. 1–11.

[15] Al-Jishi, R., and Dresselhaus, G., 1982, "Lattice-Dynamical Model of Graphite," Phys. Rev. B, **26**(8), pp. 4514–4522.

[16] Lee, C., Wei, Z., Kysar, J. W., and Hone, J., 2008, "Measurement of the Elastic Properties and Intrinsic Strength of Monolayer Graphene," Science, **321**(5887), pp. 385–388.

[17] Mott, P. H., and Roland, C. M., 2009, "Limits to Poisson's Ratio in Isotropic Materials," Phys. Rev. B, **80**(13), p. 132104.

[18] Ely, R. E., 1965, "Strength of Graphite Tube Specimens Under Combined Stress," J. Am. Ceram. Soc., **48**(10), pp. 505–508.